Journal of Statistical Physics, Vol. 62, Nos. 1/2, 1991

Monte Carlo Simulation of Phase Separation and Clustering in the ABV Model

Khwaja Yaldram[1] and Kurt Binder[2]

Received March 22, 1990; final July 27, 1990

As a model for a binary alloy undergoing an unmixing phase transition, we consider a square lattice where each site can be either taken by an A atom, a B atom, or a vacancy (V), and there exists a repulsive interaction between AB nearest neighbor pairs. Starting from a random initial configuration, unmixing proceeds via random jumps of A atoms or B atoms to nearest neighbor vacant sites. In the absence of any interaction, these jumps occur at jump rates Γ_A and Γ_B, respectively. For a small concentration of vacancies ($c_V = 0.04$) the dynamics of the structure factor $S(\mathbf{k}, t)$ and its first two moments $k_1(t)$, $k_2^2(t)$ is studied during the early stages of phase separation, for several choices of concentration c_B of B atoms. For $c_B = 0.18$ also the time evolution of the cluster size distribution is studied. Apart from very early times, the mean cluster size $\bar{l}(t)$ as well as the moments of the structure function depend on time t and the ratio Γ of the jump rates ($\Gamma = \Gamma_B/\Gamma_A$) only via a scaled time $t/\tau(\Gamma)$. Qualitatively, the behavior is very similar to the direct exchange model containing no vacancies. Consequences for phase separation of real alloys are briefly discussed.

KEY WORDS: Phase separation; clusters; Monte Carlo simulation; vacancy diffusion.

1. INTRODUCTION AND DESCRIPTION OF THE MODEL

The standard lattice models for the unmixing of binary alloys AB assume that each lattice site can be taken either by an A atom or a B atom, and unmixing is driven by a repulsive energy $\varepsilon_{AB} > 0$ which occurs if two neighboring lattice sites are taken by different kinds of atoms. Dynamics is associated to this model by assuming random exchanges of atoms in

[1] Pakistan Institute of Nuclear Science and Technology (PINSTECH), P. O. Nilore, Islamabad, Pakistan.

[2] Institut für Physik, Johannes Gutenberg-Universität Mainz, D-6500 Mainz, Germany.

0022-4715/91/0100-0161$06.50/0

nearest neighbor pairs, according to a transition probability chosen to satisfy detailed balance with the canonic distribution of states.[1-7] This model is isomorphic to the Kawasaki spin exchange kinetic Ising model[8] and clearly is not a realistic description of the dynamics of real alloys, where a direct interchange of two atoms never occurs, and interdiffusion is possible only by a vacancy mechanism.[9,10] A atoms can jump to vacant sites with a jump rate Γ_A, B atoms can jump to vacant sites with a jump rate Γ_B, if we disregard for the moment the above energy ε_{AB}. By these processes, vacancies diffuse through the lattice and thereby lead to indirect exchanges of A and B atoms (Fig. 1).

While in the standard model the parameters of interest are the reduced temperature $k_B T/\varepsilon_{AB}$, the relative concentration $c = c_B/(c_A + c_B)$ of B atoms, and the time scale as set by an exchange rate Γ_{ex} for the direct exchange of neighboring A, B atoms (in the absence of interactions), the present model contains additional parameters, namely the concentration of vacancies c_V (note $c_A + c_B + c_V = 1$), and the two jump rates Γ_A, Γ_B enter instead of Γ_{ex}. While c_V would also affect the static properties of the model already (its critical temperature, phase diagram, internal energy, etc.), this effect becomes negligibly small when $c_V \to 0$. In real alloys in thermal equilibrium, the vacancy concentration in fact is very small,[9,10] and therefore it makes sense to restrict attention to that limit. Although the static proper-

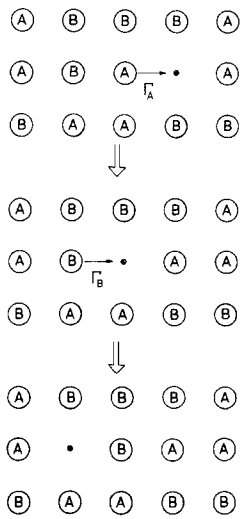

Fig. 1. Illustration of the vacancy mechanism of interdiffusion in ABV alloys on the square lattice (schematic). By suitable succession of jumps of an A atom (upper part) and a B atom (middle part), a site taken by an A atom may later be taken by a B atom (lower part).

ties of the model thus reduce to the standard model, it is not clear to what extent this is true for the dynamics: if it were true, one could introduce an effective exchange rate $\Gamma_{ex}^{eff} = c_V \Gamma_A f(\Gamma)$, where $f(\Gamma)$ is some function of the ratio $\Gamma = \Gamma_B/\Gamma_A$ of the jump rates. However, if such a mapping between the dynamical properties of the indirect exchange model and the direct exchange model did not hold, the standard application[5,11,12] of the direct exchange model of binary alloys to interpret experimental data on the unmixing of real alloys would be very doubtful.

Despite its physical significance, an extensive investigation of interdiffusion in the ABV model is available only in the noninteracting case, $\varepsilon_{AB}/k_B T = 0$.[13] There it was shown that interdiffusion occurs in general by a superposition of two exponential relaxations, and that simple proposals available in the literature to relate the interdiffusion constant to the jump rates Γ_A, Γ_B do not describe the computer simulation results accurately.

Studying the dynamics of phase separation in an ABV model with interactions, one investigates processes far from thermal equilibrium, and then even more subtle effects are conceivable: the vacancies may preferably accumulate at the interfaces between A-rich and B-rich regions, for instance. Such an effect, if it occurs, would strongly influence the mapping between the phase separation dynamics of the ABV model and the direct exchange model. Another possible effect could be a preference of the vacancies for the regions where the element with the higher jump rate predominates. If $\Gamma > 1$ and $c_A > c_B$, this could result in a "trapping" of vacancies inside isolated droplets of B atoms and a slowing down of the unmixing kinetics could result. Also, by choosing pair interactions $\varepsilon_{AA} \neq \varepsilon_{BB}$ between AA (BB) pairs, one expects different vacancy concentrations in the A-rich and B-rich regions. Such effects are outside of consideration here, however, assuming a single nonzero energy parameter ε_{AB}.

In the present work, we study the initial and intermediate stages of phase separation in the ABV model, choosing $c_V = 0.04$, $k_B T/\varepsilon_{AB} = 0.6$ and studying the relaxation of the dynamic structure factor $S(\mathbf{k}, t)$, the internal energy $E(t)$, and the distribution function $n_l(t)$ of clusters containing l B atoms as a function of time in quenching experiments that start with an initially completely random configuration of the lattice (chosen consistent with the choice of c_V and c_B, of course). In previous work on the same model[14] it was shown that the critical temperature of the model occurs at $k_B T_c$ $(c_V = 0.04)/\varepsilon_{AB} \approx 1.07$ and that for $c_V \leqslant 0.08$ the rate $\Gamma_k(t)$ of phase separation, defined as $dS(\mathbf{k}, t)/dt = \Gamma_k(t)$, depends on c_V linearly. Therefore, no systematic error is introduced by working with this vacancy concentration, although it is much larger than the vacancy concentration occurring in real alloys: it is useful to work with this relatively large value of c_V, however, since then the simulation program is reasonably fast and

in rather small lattices (linear dimensions $L=40$ and $L=80$ for $L\times L$ lattices) many vacancies are already accommodated.

In Section 2 we present numerical results for several choices of Γ between $\Gamma=0.1$ and $\Gamma=10$ and study whether by rescaling the time scale with a factor $\tau(\Gamma)$ a universal behavior is obtained. Section 3 contains a discussion and outlook for further work.

2. RESULTS OF MONTE CARLO SIMULATIONS

Standard Monte Carlo techniques[13,15,16] were used to simulate the quenching experiments, using sample averages of typically 100 runs for $L\times L$ lattices with periodic boundary conditions. The system evolves in time by randomly selecting a vacancy in the system and a randomly chosen nearest neighbor site of that vacancy with which now an exchange is attempted. If this site also is vacant, nothing happens, of course; if it is taken by an A atom or B atom, respectively, this atom jumps to the vacant

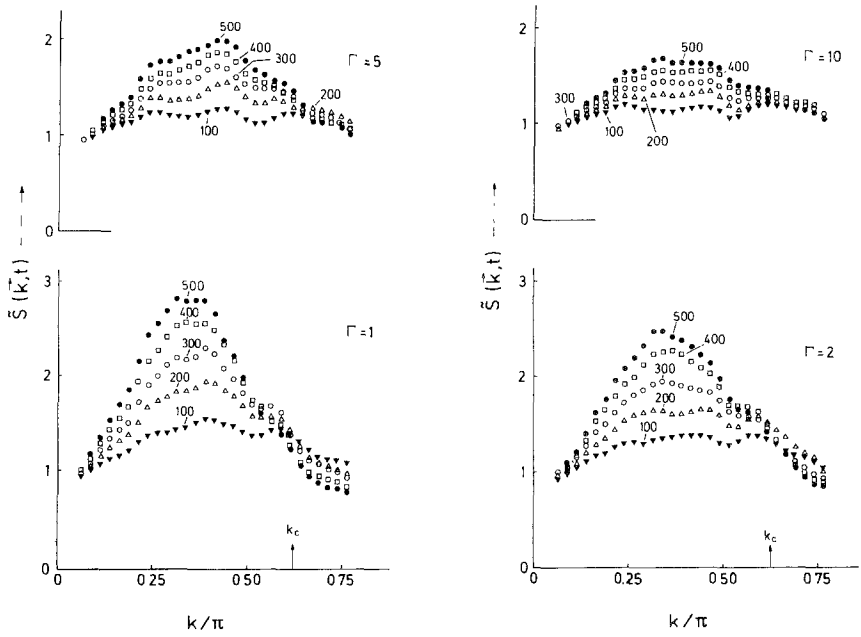

Fig. 2. Smoothed structure factor $\tilde{S}(\mathbf{k},t)\equiv\frac{1}{8}\{S(\mathbf{k}_{\nu-1},t)+3S(\mathbf{k}_\nu,t)+3S(\mathbf{k}_{\nu+1},t)+S(\mathbf{k}_{\nu+2},t)\}$ plotted vs. k_x [points are drawn at the discrete positions $\mathbf{k}'_\nu=(\mathbf{k}_\nu+\mathbf{k}_{\nu+1})/2$] for $c_A=c_B=0.48$, $c_V=0.04$, using $L=80$, and four choices of $\Gamma=1$, 2, 5, and 10. Times t after the quench are indicated. Arrow shows the mean field estimate for k_c (cf. text).

site with probability W_A or W_B, respectively. These transition probabilities are defined in terms of the energy change $\delta\mathscr{H}$ involved in the move as

$$W_A = \begin{cases} \Gamma_A & \text{if } \delta\mathscr{H} < 0 \\ \Gamma_A \exp(-\delta\mathscr{H}/k_B T) & \text{if } \delta\mathscr{H} > 0 \end{cases} \tag{1}$$

$$W_B = \begin{cases} \Gamma_B & \text{if } \delta\mathscr{H} < 0 \\ \Gamma_B \exp(-\delta\mathscr{H}/k_B T) & \text{if } \delta\mathscr{H} > 0 \end{cases} \tag{2}$$

Without loss of generality, we put the *larger* of the two jump rates Γ_A, Γ_B equal to one. Of course, necessary for the validity of the Monte Carlo algorithm is $W_A \leqslant 1$, $W_B \leqslant 1$. We then measure time in units of attempted Monte Carlo steps per vacancy. Since this algorithm is not straightforwardly vectorizable, scalar computers were used: at Mainz, we used an IBM6150 workstation, at PINSTECH, a VAX-780 computer. Figures 2 and 3 present typical results for the structure factor $S(\mathbf{k}, t)$ for $\mathbf{k}$ in the

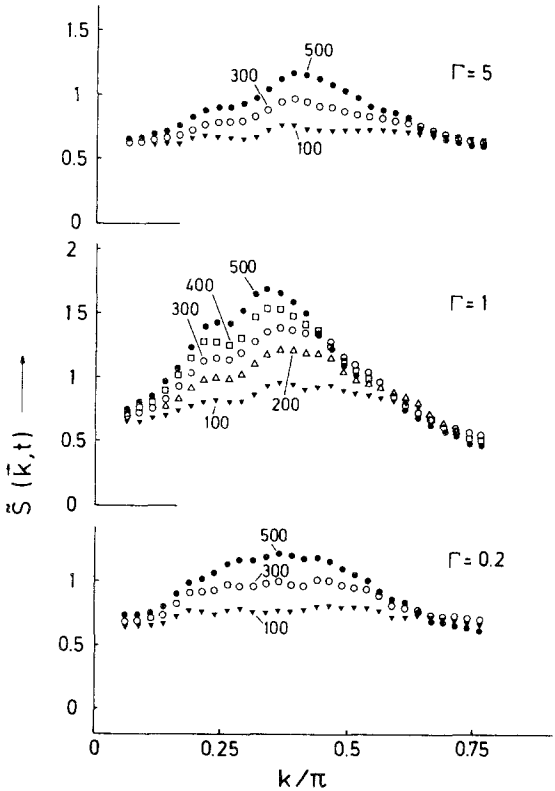

Fig. 3. Smoothed structure factor $\tilde{S}(\mathbf{k}, t)$ plotted vs. k_x and various times after the quench, for (a) $\Gamma = 5$, (b) $\Gamma = 1$, and (c) $\Gamma = 0.2$, and choosing $c_A = 0.78$, $c_B = 0.18$, $c_V = 0.04$.

lattice direction, $\mathbf{k}_v = (k_x, k_z) = (v, 0)\, 2\pi/L$, with $v = 1, 2, 3, \ldots$. Qualitatively, these data look indeed very similar to comparable results obtained for the direct exchange model.[1,3] Note that in most simulations of the direct exchange model[1–7] a circular average over the direction of $\mathbf{k}$ was used, wiping out eventual anisotropies of the square lattice. Although the Cahn–Hilliard theory[17] predicts roughly correctly[14] the range of wave vectors $(0 < k < k_c)$ over which the structure factor initially grows after the quench, this growth is much slower than exponential, and the peak position $k_m(t)$ of $S(\mathbf{k}, t)$ steadily shifts to smaller wavenumbers as the time t after the quench proceeds.

Since a direct comparison of $S(\mathbf{k}, t)$ for different values of Γ is difficult due to the statistical scatter still present in Figs. 2 and 3, we concentrate on the first two moments defined in the usual way,[1–7]

$$k_1 = \sum_k kS(\mathbf{k}, t) \Big/ \sum_k S(\mathbf{k}, t) \tag{3}$$

$$k_2^2 = \sum_k k^2 S(\mathbf{k}, t) \Big/ \sum_k S(\mathbf{k}, t) \tag{4}$$

where the direction of $\mathbf{k}$ again was chosen in the x direction of the lattice, as in Figs. 2 and 3. Figure 4a shows that in the accessible regime of times the behavior is still far from the expected law due to Lifshitz and Slyozov,[18]

$$k_1(t) \sim k_2(t) \sim t^{-a}, \qquad a = 1/3, \qquad t \to \infty \tag{5}$$

Disregarding a slight curvature that is present in the data, one could fit a power law of the form of Eq. (5) to the data, as is shown by the straight lines in Fig. 4a, but the effective exponent a^{eff} resulting from such a procedure would only be $a^{\text{eff}} \approx 0.08$, and for increasing values of Γ the effective exponent a^{eff} even would be smaller. Since in real alloys Γ is expected to be strongly temperature dependent $\{\Gamma_A = \gamma_A \exp(-E_A/k_B T),\ \Gamma_B = \gamma_B \exp(-E_B/k_B T)$, where the rates γ_A, γ_B and activation energies E_A, E_B are characteristic properties for each kind of atom, and $\Gamma = (\gamma_B/\gamma_A) \exp[-(E_B - E_A)/k_B T]$ retains an Arrhenius-like temperature dependence$\}$, changing the final temperature of a quenching experiment will mean that one also changes Γ. Observing then the relation $k_1(t)$ vs. t over a limited range of time, it is very likely that different effective exponents $a^{\text{eff}}(T)$ are found, which are physically not very meaningful, however: they only correspond to different regions of one master curve for $k_1(t)$ vs. t (Fig. 4b), which has a slight curvature extending over several decades of time, and if one analyzes data from a single decade in time only, this curvature is easily overlooked and one can fit straight lines to the log–log plot.

The analysis presented in Figs. 4a and 4b suggests that the dependence of the results on Γ can be absorbed in a rescaling of the time t into a scaled time $t/\tau(\Gamma)$, where in our case the scale factor $1/\tau(\Gamma)$ behaves as [note $\tau(\Gamma)=\tau(1/\Gamma)$ for $c_A=c_B$ because of the symmetry against interchange of A and B in this case]

$$\tau(1)\equiv 1, \qquad 1/\tau(2)=0.7, \qquad 1/\tau(5)=0.35, \qquad 1/\tau(10)=0.23 \tag{6}$$

This rescaling property is not an arbitrary "fitting phenomenon": we find that, using the same values of the scale factors in Eq. (6), also the internal energy (Fig. 5) and cluster size $\bar{l}(t)$ (Fig. 6) scale approximately. It is remarkable that this scaling property with $\tau(\Gamma)$ as given in Eq. (6) holds

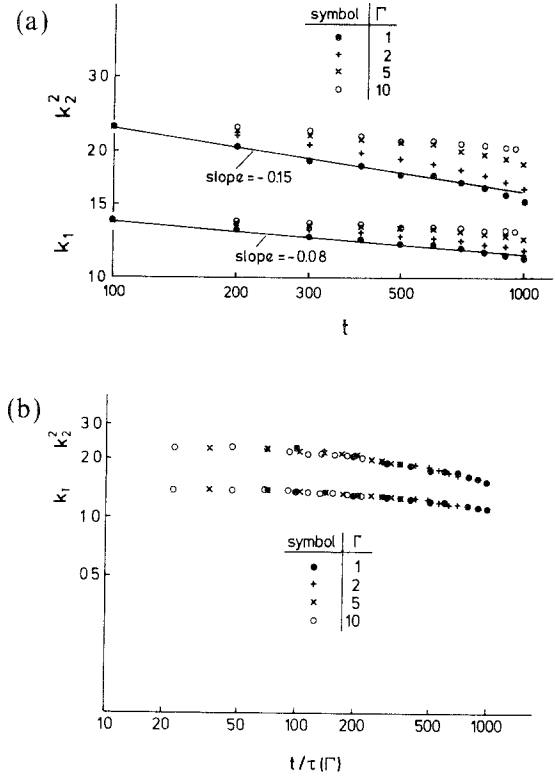

Fig. 4. (a) Log–log plot of the moments k_1 and k_2^2 vs. time t after the quench, for $c_A=c_B=0.48$, $c_V=0.04$, $L=40$, and several choices of the jump rate ratio Γ as indicated in the figure. Straight line indicates a fit to a power law for $\Gamma=1$. (b) Same as (a), but plotted against a rescaled time $t/\tau(\Gamma)$, where $\tau(\Gamma=1)\equiv 1$, $1/\tau(\Gamma=2)=0.7$, $1/\tau(\Gamma=5)=0.35$, and $1/\tau(\Gamma=10)=0.23$.

over a wide range of concentration c_A, c_B. In Fig. 5b some systematic deviation between the data for $\Gamma = 10$ and $\Gamma = 0.1$ is seen: in fact, since these data refer to $c_A \neq c_B$, there is no longer any exact symmetry property between $\tau(\Gamma)$ and $\tau(1/\Gamma)$ to be expected. Clearly, if we allowed in Fig. 5b scale factors $\tau(\Gamma)$ somewhat different from those used in Fig. 4b and quoted in Eq. (6), which are appropriate for $c_A = c_B$, a nearly perfect collapsing of the data on a master curve would be obtained. We have not done so, however, because the data for the average cluster size $\bar{l}(t)$ can be fitted with Eq. (6) rather nicely (see Fig. 6), although these data refer to exactly the same concentrations as Fig. 5 does. The scatter in Fig. 5 thus

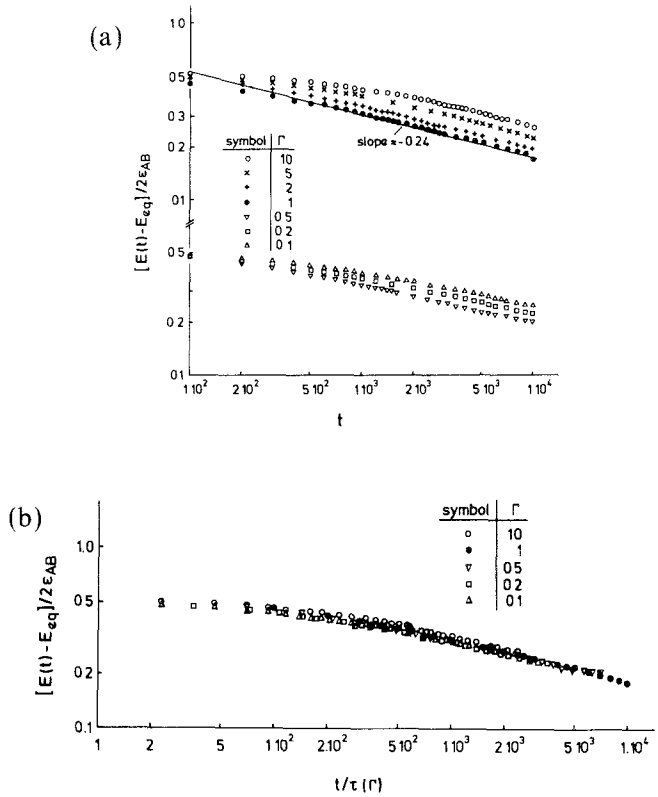

Fig. 5. (a) Log–log plot of the internal energy $E(t) - E_{eq}$, where E_{eq} is the equilibrium value of the internal energy at $k_B T/\varepsilon_{AB} = 0.6$ at the coexistence curve, as determined in ref. 14, normalized per spin in a normalization where the ABV model is transcribed to a diluted Ising ferromagnet. All data shown refer to $L = 40$, $c_A = 0.78$, $c_B = 0.18$, $c_V = 0.04$. Various choices of the jump rate are indicated. (b) Same as (a), but plotted against a rescaled time $t/\tau(\Gamma)$ using the same scaling factors $\tau(\Gamma)$ as in Fig. 4b and as quoted in Eq. (6).

may signify that either the time rescaling property is not exact or that our data still suffer somewhat from errors due to the use of too small a sample of independent runs, or both.

At this point it is important to recall that the different quantities recorded are sensitive to the long-wavelength concentration fluctuations, which are far from equilibrium in such a quenching experiment, in a somewhat different manner. E.g., in the average cluster size $\bar{l}(t)$ we have excluded clusters with sizes $l < 10$, following previous practice,[3,5]

$$\bar{l}(t) = \sum_{l \geqslant 10} \ln_l(t) \Big/ \sum_{l \geqslant 10} n_l(t) \tag{7}$$

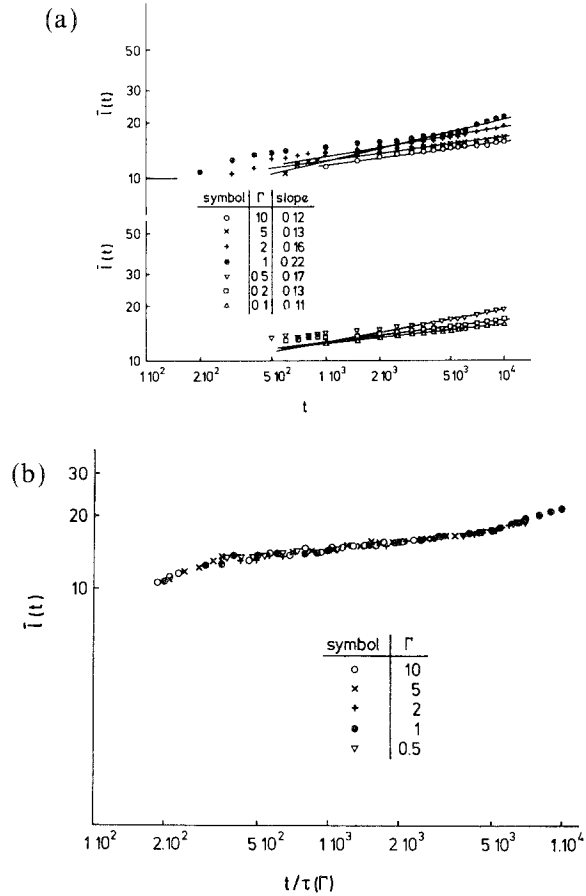

Fig. 6. (a) Log–log plot of average cluster size $\bar{l}(t)$ plotted vs. time for $L = 40$, $c_A = 0.78$, $c_B = 0.18$, $c_V = 0.04$. Various choices of the jump rate Γ are included. Straight lines indicate the power law $\bar{l}(t) \sim t^{x_{\text{eff}}}$. (b) Same as (a), but plotted against a rescaled time $t/\tau(\Gamma)$ using the scaling factors $1/\tau(\Gamma)$ as quoted in Eq. (6).

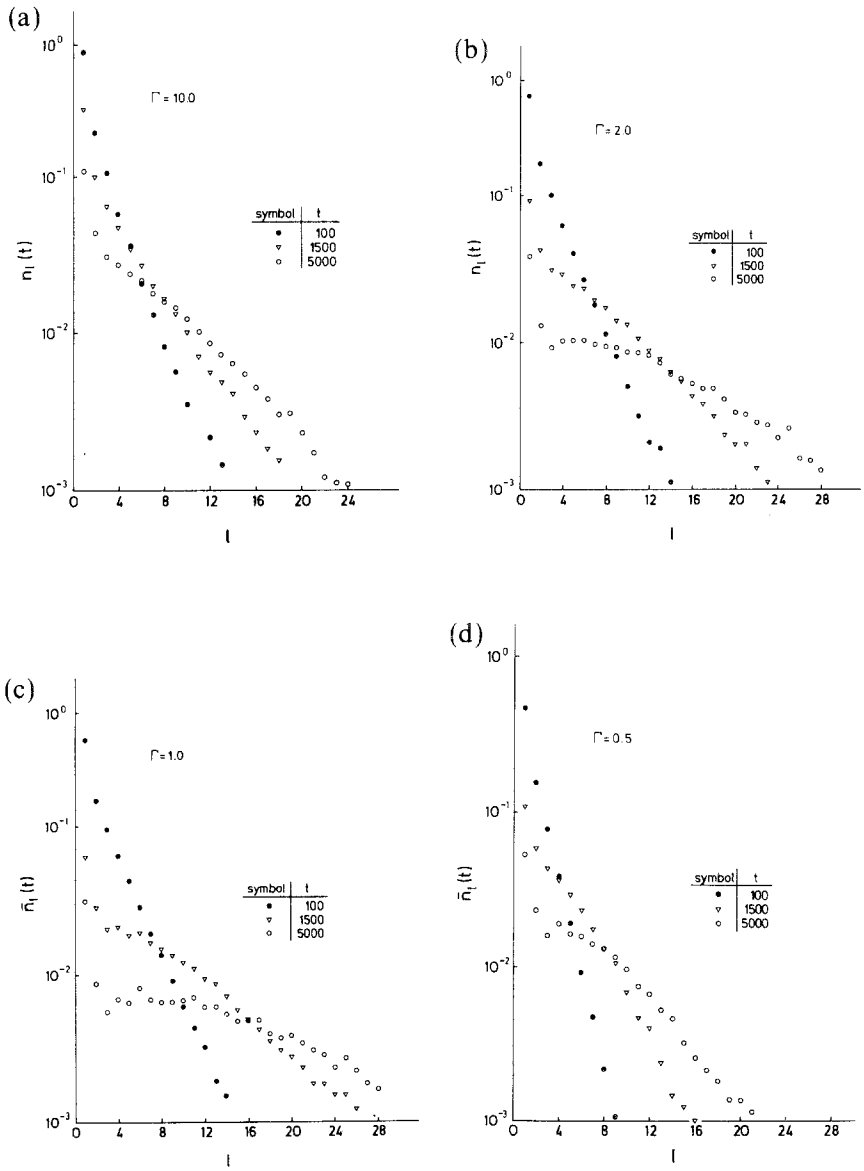

Fig. 7. Cluster size distribution $n_l(t)$ plotted vs. l for $L=80$, $c_A=0.78$, $c_B=0.18$, $c_V=0.04$, and three times t after the quench: $t=100$ (solid dots), $t=1500$ (triangles), $t=5000$ (circles). Data refer to different choices of the jump rate: (a) $\Gamma=10$, (b) $\Gamma=2$, (c) $\Gamma=1$, (d) $\Gamma=0.5$, and (e) $\Gamma=0.1$.

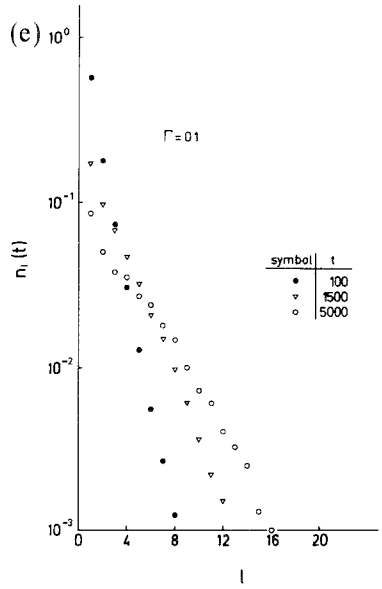

Fig. 7. (*Continued*)

$n_l(t)$ being the average number of clusters containing l B atoms at time t in the lattice, normalized per lattice site (see Fig. 7 for examples of the full distribution). Thus, small clusters do not contribute to $\bar{l}(t)$, although they are counted in the internal energy. A comparison between Figs. 7a and 7e again suggests that the relation $\tau(\Gamma) = \tau(1/\Gamma)$ is no longer an accurate approximation for an asymmetric state such as $c_A = 0.78$, $c_B = 0.18$.

A test of the time rescaling property, which is not affected by the uncertainty about the optimal choice of $1/\tau(\Gamma)$, is performed by plotting $E(t) - E_{eq}$ vs. $\bar{l}(t)$: for each value of Γ this plot is a curve, with time being a parameter of this curve. If the time rescaling property held exactly, then the curves $E(t) - E_{eq}$ vs. $\bar{l}(t)$ for the different choices of Γ would have to superpose precisely. Figure 8 shows that this is only approximately true. This property becomes very well fulfilled in the late stages of the separation process, where $\bar{l}(t)$ is large.

3. DISCUSSION

The main conclusions of this study can be summarized as follows:

(i) The qualitative characteristics of spinodal decomposition in the ABV model with a vacancy mechanism of diffusion are very similar to the AB model with the direct exchange mechanism of interdiffusion. This

conclusion is corroborated by the analysis of the time dependence of the structure factor $S(\mathbf{k}, t)$ (Figs. 2 and 3, the cluster size distribution $n_l(t)$ (Fig. 7), and snapshot pictures of the configurations (Fig. 9).

(ii) In the model with the single energy parameter ε_{AB} between A and B atoms and no other energy parameters $\varepsilon_{AA}, \varepsilon_{BB}$ etc., causing any vacancy clustering, the vacancies stay rather randomly distributed throughout the system; at least during the early and intermediate stages of phase separation, only a small enrichment of the vacancies at the interfaces between A-rich and B-rich domains is as yet observed (Fig. 9). We do not observe any significant enrichment of the vacancies in the phase with the higher jump rate.

(iii) The effect of the jump rate ratio $\Gamma = \Gamma_B/\Gamma_A$ can approximately be accounted for by rescaling the time variable with a scale factor $1/\tau(\Gamma)$. I.e., if this time rescaling property were exact, we would have

$$S(\mathbf{k}, t, \Gamma) = S(\mathbf{k}, t/\tau(\Gamma), 1) \tag{8}$$

$$E(t, \Gamma) = E(t/\tau(\Gamma), 1) \tag{9}$$

$$n_l(t, \Gamma) = n_l(t/\tau(\Gamma), 1), \qquad \bar{l}(t, \Gamma) = \bar{l}(t/\tau(\Gamma), 1) \tag{10}$$

etc. Figures 4–6 and 8 test this time rescaling property.

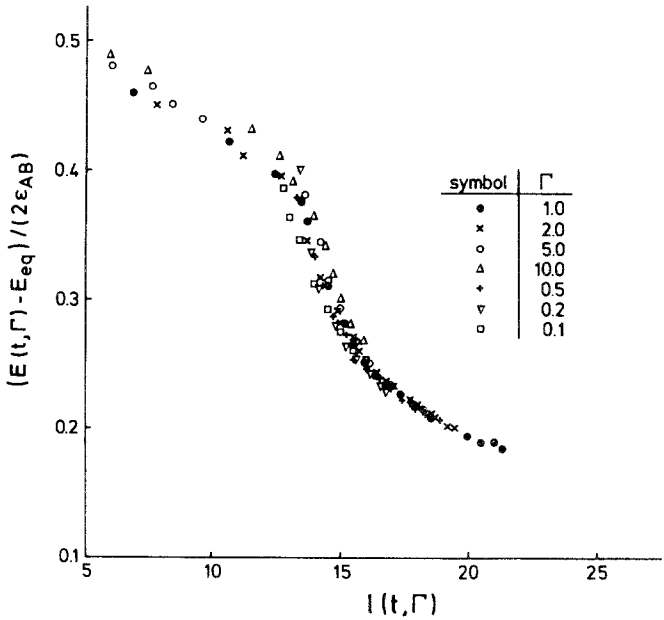

Fig. 8. Excess energy $E(t) - E_{eq}$ plotted vs. average cluser size $\bar{l}(t)$ for $L = 40$, $c_A = 0.78$, $c_B = 0.18$, $c_V = 0.04$, and various choices of Γ as indicated on the figure.

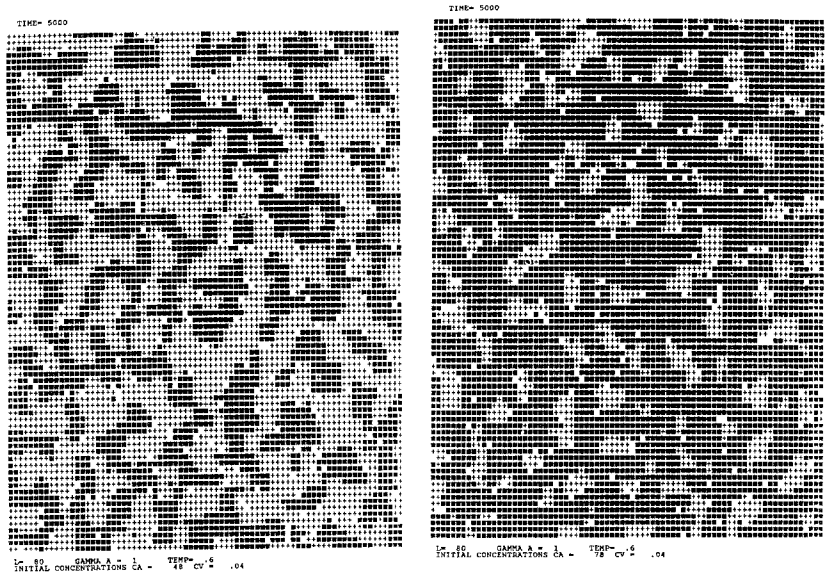

(a) (b)

Fig. 9. Typical snapshot pictures of an 80×80 lattice evolving with time for (a) $c_V = 0.04$, $c_A = c_B = 0.48$ and (b) $c_V = 0.04$, $c_A = 0.78$, $c_B = 0.18$, for $\Gamma = 1$ and a time step $t = 5000$ MCS (Monte Carlo steps) after the quench. A atoms are indicated as black squares, B atoms as crosses, and vacant sites are left blank.

(iv) The approximate numbers for the time rescaling function $1/\tau(\Gamma)$ can be rather well represented by the approximate formula

$$\tau^{-1}(\Gamma \geqslant 1) = 2(1+\Gamma)^{-1}, \qquad \tau^{-1}(\Gamma < 1) = 2(1+\Gamma^{-1})^{-1} \tag{11}$$

(see Fig. 10). Equation (11) results from the approximate description of interdiffusion in a noninteracting ABV model by the "slow mode theory,"[13] which suggests that for $c_A = c_B$ the interdiffusion constant is simply proportional to the geometric mean of the jump rates, $\Gamma_A \Gamma_B/(\Gamma_A + \Gamma_B)$. If time is measured in units of the larger jump rate and $\Gamma_B > \Gamma_A$, this means that the interdiffusion constant is $\Gamma_A/(\Gamma_A + \Gamma_B) = 1/(1+\Gamma)$; if $\Gamma_B < \Gamma_A$, however, the interdiffusion constant is $\Gamma_B/(\Gamma_A + \Gamma_B) = 1/(\Gamma^{-1} + 1)$. Thus, Eq. (11) results if we choose a normalization $\tau(1) \equiv 1$. Note that the slow mode theory does not describe interdiffusion accurately even in thermal equilibrium; thus, it is not expected that Eq. (11) holds true exactly. In addition, during phase separation at the considered temperatures the system develops rather rapidly from $c_A = c_B$ to separate regions of almost pure A and pure B. There is no reason that a theory

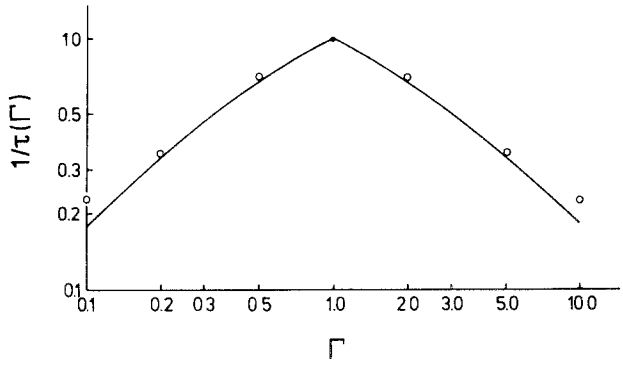

Fig. 10. Time scaling factor $\tau^{-1}(\Gamma)$ plotted vs. Γ for $c_A = c_B$ (circles) and approximate theoretical prediction $\tau^{-1}(\Gamma > 1) = 2(1+\Gamma)^{-1}$, $\tau^{-1}(\Gamma < 1) = 2(1+\Gamma^{-1})^{-1}$ (curve).

addressing nearly homogeneous states close to equilibrium, as considered in ref. 13, is at all relevant to the intermediate or later stages of unmixing, where the system is very inhomogeneous and far from equilibrium. Thus, the approximate validity of Eq. (11) shown in Fig. 10 really comes as a surprise.

A rather nontrivial behavior is expected, of course, if one of the rates gets much smaller than the other one; in particular, we expect that then the possible percolation of one component (or both components A, B in three dimensions) will have a marked effect on the phase separation kinetics. This behavior is outside the scope of the present study, however.

ACKNOWLEDGMENTS

This work was started while one of us (K.Y.) was visiting the University of Mainz in the framework of the PAEC–KFK collaborative project; support from this project is gratefully acknowledged. We are grateful to Prof. K. W. Kehr for supplying us with the simulation program of ref. 13 for the random ABV model, which was extended to the present interaction model. Thanks are due to the IBM Deutschland GmbH for supplying us with an IBM6150 workstation which was used for parts of this work, in the framework of the Studienvertrag No. F123, and to Dipl. Phys. N. Pistoor for helpful advice with this workstation. The help of M. Dad in the development of the program for the cluster size distribution is gratefully acknowledged. Finally, useful discussions with Dr. A. Sadiq and Prof. K. W. Kehr are gratefully acknowledged.

REFERENCES

1. A. B. Bortz, M. H. Kalos, J. L. Lebowitz, and M. A. Zendejas, *Phys. Rev. B* **10**:535 (1974).
2. J. Marro, A. B. Bortz, M. H. Kalos, and J. L. Lebowitz, *Phys. Rev. B* **12**:2000 (1975).
3. M. Rao, M. H. Kalos, J. Marro, and J. L. Lebowitz, *Phys. Rev. B* **13**:4328 (1976); A. Sur, J. L. Lebowitz, J. Marro, and M. H. Kalos, *Phys. Rev. B* **15**:536 (1977); M. H. Kalos, J. L. Lebowitz, O. Penrose, and A. Sur, *J. Stat. Phys.* **18**:39 (1978).
4. J. Marro, J. L. Lebowitz, and M. H. Kalos, *Phys. Rev. Lett.* **43**:282 (1979).
5. K. Binder, M. H. Kalos, J. L. Lebowitz, and J. Marro, *Adv. Colloid Interface Sci.* **10**:173 (1979).
6. J. L. Lebowitz, J. Marro, and M. H. Kalos, *Acta Met.* **30**:297 (1982).
7. J. G. Amar, F. E. Sullivan, and R. D. Mountain, *Phys. Rev. B* **37**:196 (1988).
8. K. Kawasaki, in *Phase Transitions and Critical Phenomena*, Vol. 2, C. Domb and M. S. Green, eds. (Academic Press, 1972), Chapter 11.
9. J. R. Manning, *Diffusion Kinetics for Atoms in Crystals* (Van Nostrand, Princeton, New Jersey, 1968).
10. C. P. Flynn, *Point Defects and Diffusion* (Clarendon Press, Oxford, 1972).
11. J. D. Gunton, M. San Miguel, and P. S. Sahni, in *Phase Transitions and Critical Phenomena*, Vol. 8, C. Domb and J. L. Lebowitz, eds. (Academic Press, 1983), p. 267.
12. K. Binder, in *Alloy Phase Stability*, A. Gonis and L. M. Stocks, eds. Kluwer, Dordrecht, 1989), p. 232; in *Phase Transformations in Materials*, P. Haasen, ed. (VCH Verlagsgesellschaft, Weinheim, in press), Chapter 7.
13. K. W. Kehr, K. Binder, and S. M. Reulein, *Phys. Rev. B* **39**:4891 (1989).
14. K. Yaldram and K. Binder, *Acta Met.* (in press).
15. K. Binder and D. W. Heermann, *Monte Carlo Simulation in Statistical Physics—An Introduction* (Springer, Berlin, 1988).
16. K. W. Kehr and K. Binder, in *Applications of the Monte Carlo Method in Statistical Physics*, K. Binder, ed. (Springer, Berlin, 1987), p. 181.
17. J. W. Cahn and J. E. Hilliard, *J. Chem. Phys.* **28**:258 (1958); **31**:688 (1959); J. W. Cahn, *Acta Met.* **9**:795 (1961); *J. Chem. Phys.* **42**:93 (1965).
18. I. M. Lifshitz and V. V. Slyozov, *J. Phys. Chem. Solids* **19**:35 (1961).